32ND INTERNATIONAL COSMIC RAY CONFERENCE, BEIJING 2011

PAMELA measurements of boron and carbon spectra in the energy range 100 MeV/n - 100 GeV/n

CRISTIAN DE SANTIS[1,2], ON BEHALF OF THE PAMELA COLLABORATION
[1]*INFN, Sezione di Roma - Tor Vergata, I-00133 Rome, Italy*
[2]*University of Rome - Tor Vergata, Department of Physics, I-00133 Rome, Italy*
cristian.desantis@roma2.infn.it

Abstract: Accurate measurements of the elemental composition of cosmic rays over a wide energy range are required in order to understand the origin, propagation and lifetime of the cosmic radiation.
The primary cosmic rays (e.g. C and O), produced at the sources, propagate through the interstellar medium giving information about the composition at the source. Secondary elements (e.g. Li, Be, and B) are tracers of amount of matter traversed by the cosmic rays.
PAMELA (Payload for Antimatter Matter Exploration and Light nuclei Astrophysics) is a satellite-borne experiment devoted to the study of the cosmic radiation over a wide energy range.
The scientic objectives addressed by the mission are the measurement of the anti-protons and positrons spectra in cosmic rays, the hunt for anti-nuclei as well as the determination of light nuclei fluxes from hydrogen to oxygen in a wide energy range and with high statistics.
New results on the boron and carbon spectra in the energy range 100 MeV/n - 100 GeV/n will be presented.

Keywords: cosmic rays

1 Introduction

Measurements of the elemental composition of cosmic rays over a wide energy range are required in order to understand the origin, propagation and lifetime of the cosmic radiation.
The primary cosmic rays (e.g. C and O), produced at the sources, propagate through the interstellar medium giving information about the composition at the source. Secondary elements (e.g. Li, Be, and B) are tracers of amount of matter traversed by the cosmic rays.
Abundances of secondary light nuclei (Li, Be and B) in cosmic rays are due to spallation of carbon and oxygen nuclei as they traverse the interstellar hydrogen. The amount of these elements determines the average thickness of interstellar matter which the radiation traverses and indicates an average lifetime of the cosmic rays in the galaxy of about 3 million years. Energy spectra of Li, Be and B are steeper than those of C and O, indicating that at higher energies nuclei do not undergo so much fragmentation, presumably because they leak out of the galaxy sooner than those lower energy [1], [2], [3], [4].
PAMELA (a Payload for Antimatter Matter Exploration and Lightnuclei Astrophysics)[5] is measuring the light nuclei component, up to oxygen, of the cosmic radiation since July 2006. The hydrogen and helium spectra have already been released [6] and are presented elsewhere in this conference [7]. Also lithium and beryllium spectra are presented elsewhere in this conference [8]. In this paper, preliminary energy spectra of cosmic-ray boron and carbon nuclei are presented and compared with other measurements.

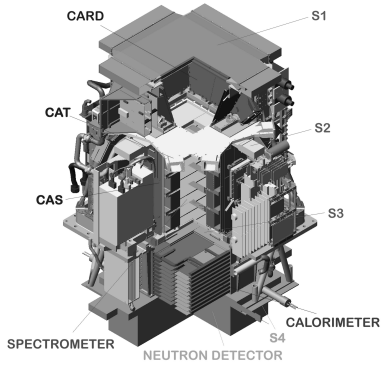

Figure 1: schema of the PAMELA apparatus.

2 The PAMELA Apparatus

The PAMELA apparatus is housed inside a pressurized container attached to the Russian Resurs-DK1 satellite,

which was launched on June 15th 2006. The orbit is elliptical and semi-polar, with an inclination of 70.0° and an altitude varying between 350 km and 610Km.
PAMELA comprises (from top to bottom as shown in Figure 1): a time-of-flight (ToF) system (S1, S2, S3), a magnetic spectrometer with silicon tracker planes, an anticoincidence system (CARD, CAT, CAS), an electromagnetic imaging calorimeter, a shower tail catcher scintillator (S4) and a neutron detector.

2.1 Time of Flight

The scintillator system provides trigger, charge and timeof-flight information. There are three scintillators layers, each composed of two orthogonal planes, divided into paddles (8 for S11, 6 for S12, 2 for S21 and S12 and 3 for S32 and S33).

2.2 Magnetic Spectrometer

The magnetic spectrometer is built around a permanent magnet composed of 5 blocks of segmented Nd-Fe-B alloy with a residual magnetization of 1.3 T. The size of the magnetic cavity is $13.1 \times 16.1 \times 44.5 cm^3$, with a mean magnetic field of 0.43 T. Six layers of 300 μm thick double-sided microstrip silicon detectors are used to measure particle deflection.

2.3 Anticoincidence System

Plastic anticoincidence scintillators allows to reject spurious triggers due to particles interacting with the body of the satellite. The CARD anticoincidence system comprises four 8 mm thick scintillators which bound the volume between S1 and S2. The CAT scintillator is placed on top of the magnet and has a central rectangular aperture corresponding to the magnet cavity. Four scintillators, arranged around the magnet, form the CAS lateral anticoincidence system.

2.4 Elctromagnetic Imaging Calorimeter

The silicon tungsten sampling calorimeter provides topological and energetic information for particles which generate showers in the calorimeter, allowing lepton/hadron discrimination [9] and precise measurement of the energy of impinging electrons and positrons [10]. The calorimeter comprises 44 single-sided silicon planes (made of nine 380 μm thick, $8 \times 8 cm^2$ wide sensors) interleaved with 22 plates of tungsten absorbers, for a total depth of $16.3 X_0$ (0.6 nuclear interaction lengths).

2.5 Shower Tail Scintillator

This scintillator ($48 \times 48 \times 1 cm^3$) is located below the calorimeter and is used to improve hadron/lepton discrimination by measuring the energy not contained in the calorimeter and as a stand-alone trigger for the neutron detector.

2.6 Neutron Detector

The $60 \times 55 \times 15 cm^3$ neutron detector is composed of 36 ^3He tubes arranged in two layers and surrounded by polyethylene shielding and a U shaped cadmium layer to remove thermal neutrons not coming from the calorimeter. It is used to improve lepton/hadron identification by detecting the number of neutrons produced in the hadronic and electromagnetic cascades.

3 Data Analysis

3.1 Detector Characteristics

3.1.1 Geometrical Factor

The geometrical factor (G_f) of PAMELA has been evaluated by defining a fiducial area 0.15 cm from the walls of the magnetic cavity. Only particles passing through this fiducial volume, which ensures that all particles entering the magnetic cavity can cross the trigger scintillators without impinging on the magnet walls, have been selected for analysis. The derived value of $G_f = 19.85 cm^2 sr$ has been found to be constant above 1 GV within 0.1%.

3.1.2 Trigger System

In low radiation regions the trigger is defined by coincidences between at least one of the two planes of the three scintillator systems (S1, S2, S3). In high latitude regions or inside the radiation belts, where the particle rate is higher, S1 plane is excluded from the trigger condition and a coincidence of all ToF layers of S2, S3 is required.

3.1.3 Live Time

The live time t_{live} has been evaluated using the trigger system. Counters for the live and dead time (t_{live}, t_{dead}) have been cross-checked with the on-board time of the CPU allowing the acquisition time (t_{acq} = t_{live}+t_{dead}) to be determined.

3.2 Event Selection

3.2.1 Correction at the top of the payload

Flux attenuation has been estimated with simulation. The resulting correction factor, which accounts for non-elastic interactions and for the loss (gain) of particles from (within) the acceptance due to elastic scattering, is constant above 1 GV and amounts to $\simeq 22\%$ for boron and $\simeq 20\%$ for carbon due to their differing cross-sections.

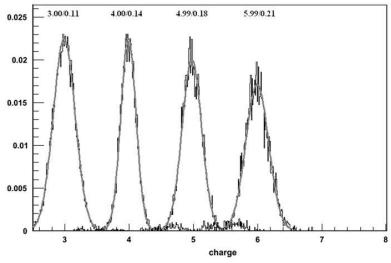

Figure 2: Charge separation in the ToF system. The histograms are normalized to the number of events. The Gaussian fit of the peak gives the detector charge resolution.

3.2.2 Trigger selection

Timing information from the ToF scintillator paddles has been used to evaluate the β of the particle. Albedo particles crossing PAMELA from bottom to top have been discarded by requiring $\beta > 0$. No anticoincidence cut has been used.

3.2.3 Boron and Carbon Selection

Charge Identification The energy loss of a charged particle traversing matter is described by the Bethe-Bloch equation, $\frac{dE}{dx} \propto \frac{Z^2}{\beta^2}$ (neglecting logarithmic terms). A measurement of the average energy released the ToF planes for a given event at a given rigidity can therefore be used to distinguish between different particles. Boron and carbon candidates have been selected requiring energy loss compatible with Z=5 and Z=6 nuclei in each layer of a given combination (S12,S2,S3) of ToF planes. In Figure 2 the charge separation in the ToF system is shown.

Charge Identification Efficiency The charge identification efficiency has been estimated by selecting a sample of events by means of S11 and the calorimeter. The overall efficiency of the selection has been evaluated for each rigidity bin R_i and has been found to exceed 65% at a few GV, decreasing gradually at lower rigidities due to saturation effects.

3.2.4 Geomagnetic Selection

The local geomagnetic cutoff *G* has been evaluated using the Störmer approximation [11]. A value of $G = 14.9/L^2$ - valid for vertically incident particles - has been estimated using the IGRF magnetic field model along the orbit; from this the McIlwain L shell has been calculated [12]. Particles have been selected requiring $R > 1.3G$.

3.2.5 Tracker Selection

Track Fitting Particle rigidity has been obtained from the fit of the track in the spectrometer. Only events with a single track fully contained inside the fiducial acceptance have been selected. For each particle, the tracking system provided up to 12 position measurements (6 in the bending view), which have been interpolated to form a trajectory described by integrating the equations of motion in the magnetic field. An event has been selected if the fit of the track had a good χ^2, with an energy dependent selection tuned on experimental data in order to obtain a constant efficiency of 85%. This resulted in a higher $\chi 2$ at low energies due to larger multiple scattering effects.
Spectra have not been unfolded.

Track Fitting Efficiency Due to the low statistics in flight data, the tracker efficiency has been estimated by means of simulations. Extensive Monte Carlo simulations have been carried out in order to estimate with low statistical errors the efficiency of the selections. The simulated boron sample consists a mixture (35%^{10}B+65%^{11}B) in order to mimic the boron isotopic composition in cosmic rays. For carbon a pure ^{12}C sample ha been used neglecting any contribution from ^{13}C. The overall efficiency of the various selections has been evaluated for each rigidity bin R_i and has been found to be almost constant in the whole rigidity range both for boron and carbon. Since the estimate of the track efficiency relied on a simulation of the apparatus, which for the spectrometer accounted for the measured noise of each silicon plane and performance variations over the duration of the measurement, the simulation code has been validated by comparing the distributions of several significant variables (e.g. coordinate residuals, chi-squared and the covariance matrix from the track fitting) with those obtained from real data. The estimated contribution of the relative positions of the tracking sensors (incoherent alignment) has been accounted in the validation procedure.

4 Results

In Figure 3 and Figure 4, filled circles show the preliminary energy spectra of boron and carbon measured by PAMELA in the energy range 100 MeV/n - 100 GeV/n. The error bars represent the statistical error; if not visible, they lie inside the data points. In Figure 3 the measurements of HEAO (open crosses) [4], HEN (open triangles) [1] and Orth et al. (open boxes) [2] are also show in the plot. The measurements of HEAO (open crosses) [4] and CREAM (open boxes) [13],[14].
The preliminary results reported here are in good agreement with those of other experiments. Additional work is in progress to improve the current results, including the unfolding of the finite resolution of the spectrometer and addressing the effects of secondary particles from interactions in the pressurized vessel.

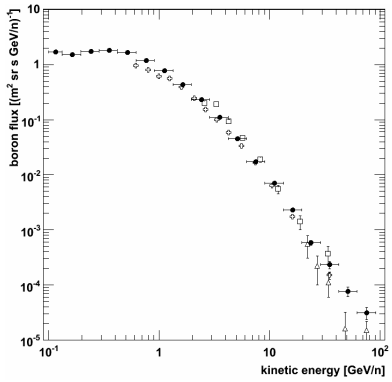

Figure 3: the boron spectrum measured by PAMELA (filled circles) compared with selected previous data. Open crosses, open triangles and open boxes represent the measurements of HEAO, HEN and Orth et al., respectively.

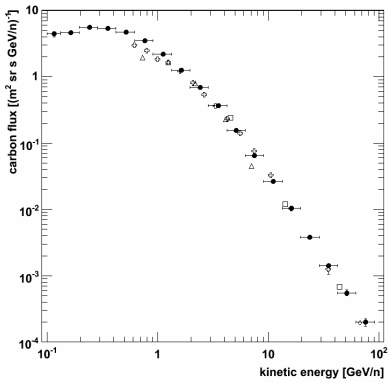

Figure 4: the carbon spectrum measured by PAMELA (filled circles) compared with selected previous data. Open crosses and open boxes represent the measurements of HEAO and CREAM, respectively.

5 Summary

Preliminary energy spectra of boron and carbon measured by PAMELA have been presented. The results are in agreement with other observations in the energy range 100 MeV/n - 100 GeV/n. An analysis work of the elemental spectra of other cosmic-ray nuclei, including lithium, beryllium and oxygen is still in progress.

6 Acknowledgements

This work is supported by The Italian Space Agency (ASI), Deutsches Zentrum für Luft- und Raumfahrt (DLR), The Swedish National Space Board, The Swedish Research Council, The Russian Space Agency (Roscosmos) and The Russian Foundation for Basic Research.

References

[1] E. Juliusson, Astrophysical Journal, 1974, **191**: 331-348
[2] Orth, C. D. et. al., Astrophysical Journal, 1978, **226**(1): 1147-1161
[3] Swordy, S. P. et. al., Astrophysical Journal, 1990, **349**(1): 625633
[4] Engelmann, J. J. et. al., Astronomy and Astrophysics, 1990, **233**(1): 96-111
[5] Picozza, P. et. al., Astroparticle Physics, 2007, **27**(4): 296-315
[6] Adriani, O. et al., Science, 2011, **332**(6025): 69-72
[7] Casolino, M. et al., Recent PAMELA measurements of proton and helium nuclei and cosmic ray acceleration in the galaxy, in this conference
[8] Menn, W et al., Measurements of Cosmic-Ray Lithium and Beryllium Isotopes with the PAMELA-Experiment, in this conference
[9] Boezio, M. et al., Astroparticle Physics, 2006, **26**(2): 111-118
[10] Boezio, M. et al., Nuclear Instruments and Methods in Physics Research Section A, 2002, **487**(3): 407-422
[11] Shea, M. A. et al., Physics of the Earth and Planetary Interiors, 1987, **48**(3-4): 200-205
[12] International geomagnetic reference field, Tech. rep., IAGA (2005)
[13] Wakely, S. P. et al., Advances in Space Research, 2008, **42**(3): 403-408
[14] Maestro, P. et al., Nuclear Physics B Proceedings Supplements, 2009, **196**: 239-242